P157 Retrieval of Carbon Monoxide in Troposphere with Satellite Infrared Radiometer

Fumie Kataoka[1*], Yasushi Mitomi[1],

[1]Remote Sensing Technology Center of Japan, Ibaraki, Japan

1. INTRODUCTION

In recent year, air pollution caused by developing country has become a serious problem. Especially, China has been achieving explosive growth, which gives a lot of pollutants to the atmosphere. Some report said that these pollutants flow to Japan, and even travel to North America.

But, this is not all China's fault. Because China is now accepting a lot of foreign-capitalized factory and China's market has also been making a wonderful progress of technology like clean-burning and energy-saving.

Now, we investigate latest condition of atmosphere across East Asia. Especially, we focused on carbon monoxide (CO) concentration in troposphere which is mainly attributed to our economic activity. CO is oxidized by reacting with OH radicals and produce anthropogenic ozone in the presence of nitrogen oxides (NOx). Tropospheric ozone has an affect on the human body, forest and crops as a phenomenon of photochemical oxidant of smog. Furthermore, it also effect global warming, because it has an important role to determine the concentration of greenhouse effect gases like a methane, carbon dioxide and halocarbon.

In this study, we analyzed a spatiotemporal dynamics of CO in East Asia and investigated the correlation with tropospheric ozone using TES product (Tropospheric Emission Spectrometer). TES was launched on NASA's EOS Aura satellite in July 2004 .

In the troposphere, atmospheric disturbance is so active that the monitoring of atmospheric condition at fine intervals is very important. We will further discuss the possibility of temporal-spatial higher-accuracy dataset creation using other satellite.

2. SATELLITE DATA

The Tropospheric Emission Spectrometer (TES) measures global distribution of atmospheric pollutants with revisit of 16 days. TES aboard on Aura satellite which is one of the A-train (Afternoon around 1:30pm equator crossing). TES sensor (Fourier-transform spectrometer) covers the spectral range of 650–3050 [cm^{-1}] at an apodized spectral resolution of 0.1 [cm^{-1}] (nadir viewing).

----

* *Corresponding author address:* Fumie Kataoka, Remote Sensing Technology Center of Japan, Tsukuba-Mitsui BLDG 18F, 1-6-1 Takezono, Tsukuba-city, Ibaraki, 305-0032, JAPAN ; e-mail: kataoka.fumie@restec.or.jp.

Table 1 shows retrieval species of TES product and observational mode. TES Level 2 products contain retrieved gas and temperature profiles (67 pressure levels) at the observation points. Level 3 product represents global surveys at spacing of 2 degrees latitude and 4 degrees longitude with 16 pressure levels. These data consists of 16 consecutive orbits with 2 days cycle.

Table1. TES product spices types and viewing mode.

Species	H_2O	O_3	CH_4	CO	HNO3	HDO	AtmT
Nadir Swath Object	X	X	X	X	-	X	X
Limb Swath Object	X	X	-	-	X	X	X

3. DATA ANALYSIS

CO levels in Northern hemisphere maximize during winter-spring. During these seasons, CO is emitted from active burning of fossil fuel or biomass burning in East Asia. As noted above, CO induced the formation of tropospheric ozone expressed following chemical equation.

$$\begin{aligned} &CO + OH \xrightarrow{O_2} CO_2 + HO_2 \\ &HO_2 + NO \rightarrow OH + NO_2 \\ &NO_2 + h\nu \xrightarrow{O_2} NO + O_3 \end{aligned} \quad (1)$$

CO reacts with OH radicals and produces HO_2. In the presence of sufficiently mixing ration of NO, HO_2 converts NO to NO_2. Continuously, NO_2 produces ozone through the reaction of photo-dissociation.

These reactions of the formation of ozone are expressed by net chemical equation.

$$CO + 2O_2 \rightarrow CO_2 + O_3 \quad (2)$$

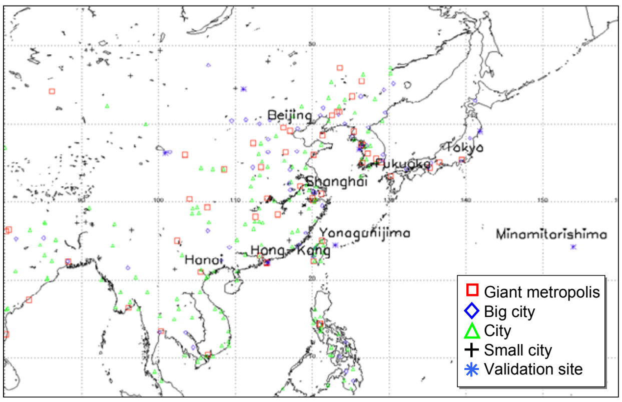

Figure 1. The target domain and some major cities.

So we focused on these seasons in recent year from 2006 to 2009 and analyzed the current conditions of Asian atmosphere.

3.1 *TEMPORAL EVALUATION*

3.1.1 *REGIONAL SCALE*

Figure 2 shows the monthly mean CO concentration at surface in January-May from 2006 to 2009. These figures also plot the point where reach high-level of CO (exceed 300 ppbv) in lower troposphere (lower than 850 hPa) which data is sourced from TES Level 2 product.

Throughout the months of January until March, high concentration site is found across the land in East Asia. In particular, East China with a number of mega cities and Indochina are markedly high. The latter area, January-April period fall during the dry season and it induce a biomass burning.

The level of CO in 2007 is noticeable in the period of four years. It also shows a decrease of the emergence of high concentration in recent year.

3.1.2 *SPECIFIC SITE*

We focus on some major cities and validation site shown in Figure 1. Figure 3 show the time-pressure cross section of CO in January-May from 2006 to 2009.

In the big city like Shanghai, Hong-Kong and Hanoi, high concentration of CO exceed 300 ppbv in lower troposphere is occasionally found. However, the other side of the East China Sea such as Fukuoka, Tokyo, Yonagunijima and Minamitorishima is not so frequently and the level of CO decreases with distance from Asian continent. But some case, the latter areas show a high level CO at the same time or later as the peak in the former area. It indicates possibility of cross-border pollution. SO, we pick up an obvious case and approach the transport of continental pollution.

Before that, we compare TES Level3 and in-situ data (provided by Japan Meteorological Agency) at two validation sites in January-May from 2006 to 2009. Figure 4 shows the comparative result at Yonagunijima and Minamitorishima. It seems like TES level3 is slightly low because the level3 data is interpolated in grid interval and the sensitivity of surface is not so high, but these data is basically consistent.

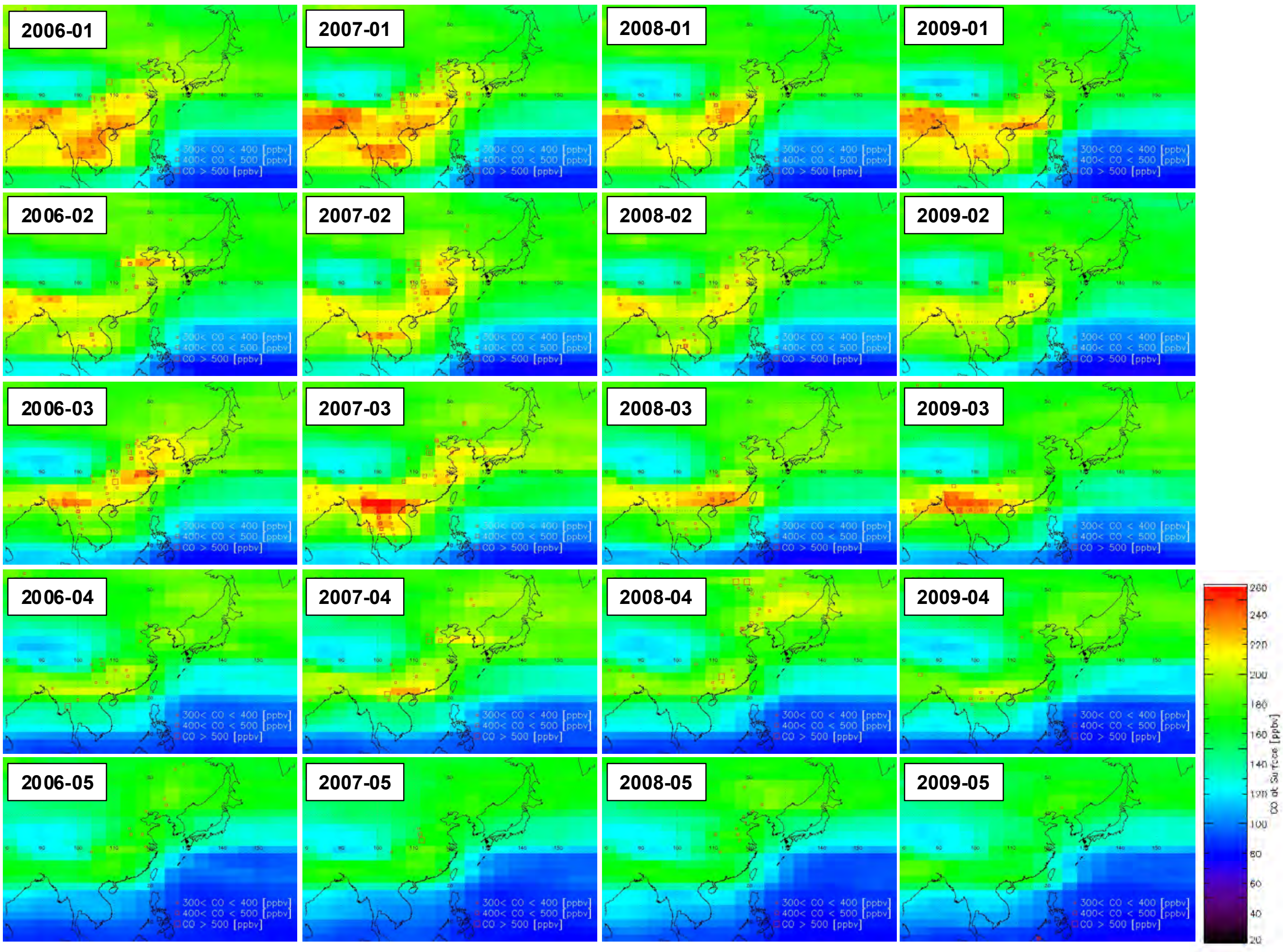

Figure 2. Monthly mean CO concentration at surface in January-May from 2006 to 2009.The high concentration of CO in lower troposphere (lower 850 [hPa]) is plotted over each figure.

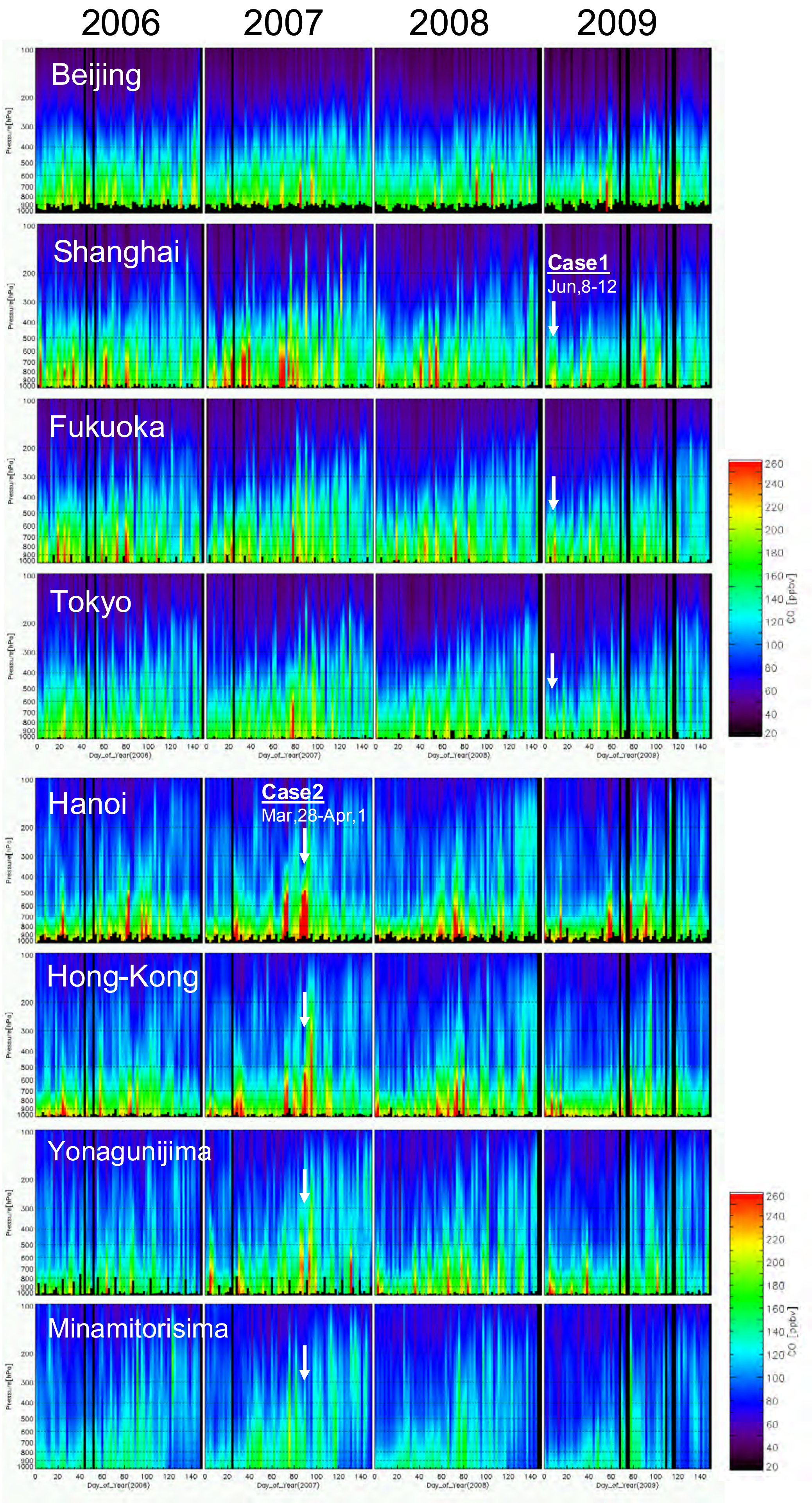

Figure 3. The time-pressure cross section of CO in January-May from 2006 to 2009.These figure shows the daily profile from 1000 [hPa] to 100 [hPa].

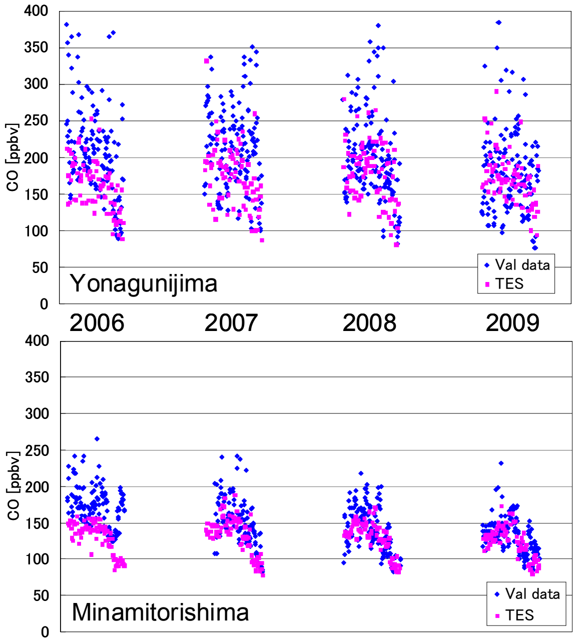

Figure 4. The comparison of TES level3 CO product and in-situ data in January-May from 2006 to 2009 at Yonagunijima (above) and MInamitorishima (below).

3.2 *SPATIAL EVALUATION*

In order to investigate the possibility of cross-border pollution, we focused two latitudinal belts shown in Figure5.

zone1: around 35° N (108 – 144°E)
zone2: around 23° N (100 – 156°E)

Each belt has the source of anthropogenic pollutant emission in Asian continent. One is East China, the other is Indochina. We attempted to instantiate the possibility of cross-border pollution sourced from these areas using following cases (indicate by arrows in Figure 3).

case1: January 8, 2009 - January 12, 2009 (zone1)
case2: March 28, 2007 - April 1, 2007 (zone2)

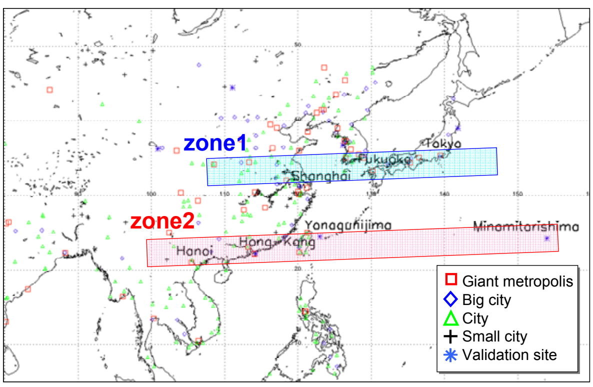

Figure 5. The rectangle shows analytical zone. Zone1 covers around 35° N and zone 2 around 23° N.

テェ mechanism of pollutant transport from the Asian boundary layer is presented by some report (Liang et al., 2004 and Turquety et al.,2008). The export of pollutants is proposed the following processes (Figure 6).

1) transport behind cold front
2) warm conveyor belt lifting
3) convective lifting
4) orographic forcing

And the exported pollutant from Asia is transported by westerly winds or occasionally by mountain waves.

3.2.1 *CASE 1 (January 8, 2009 - January 12, 2009)*

Figure 7(a) show the longitude-time cross sections of CO and ozone for latitudinal band (zone1) on alternate days. These representations show that the high concentration of CO is eastward-flowing from East China (Nanjing, Shanghai and Kwangju) to Japan. In keeping with this trend, the lower tropospheric ozone also increases the level, especially in January 10, 2009.

On January 8 and 9, the cyclone grew intensely in the southern coasts of Japan and moved eastward. The cyclone was brought the high concentration of CO from East China. This case corresponds to the export process 1). As shown in Figure 7(b), in almost all layer of troposphere, westerly wind was blowing at Nanjing, Shanghai and Fukuoka. This mid-latitude westerly promoted the transport of CO and even induced an anthropogenic ozone genesis.

3.2.2 *CASE 2 (March 28, 2007 - April 1, 2007)*

The longitude-time cross sections of CO and ozone for latitudinal band (zone2) shown in Figure 8(a). CO cross section shows the two source contributions. One is northern part of Indochina, the other is near the Taiwan.

Indochina fell during the dry season at this time. Figure 8(b) shows the MODIS CMG (Climate Modeling Grid) Fire product (MYD14C8H) in East Asia. This product is gridded statistical summaries of fire pixel information intended for used in regional and global modeling, and are generated at 0.5 degree grid for the time periods of 8 days. During period 1 and 2, the northern part of Indochina counted more than 100 times fire detection per pixel in contrast with period 3.

On March 27, the cyclone with front moved eastward in the East China Sea and following this, the moving High from continent appeared. The down-stream wind in Hanoi, Hong-Kong and Ishigakijima (near Yonagunijima) blew southwesterly toward the anticyclone as shown in Figure 8(c). This case is thought to be a compound export process of 1) and 2). These southwesterly wind transported the biomass burning-derived CO and induced extensive ozone genesis in lower troposphere. The high level of ozone also reached Minamitorishima on Apr. 1.

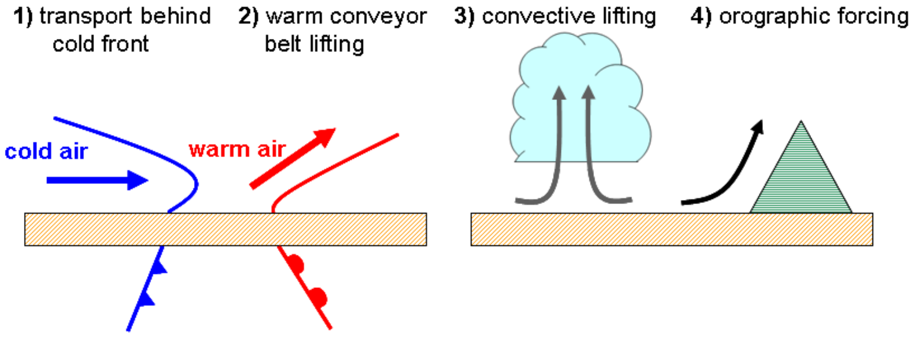

Figure 6. The schematic draw of pollutant export process.

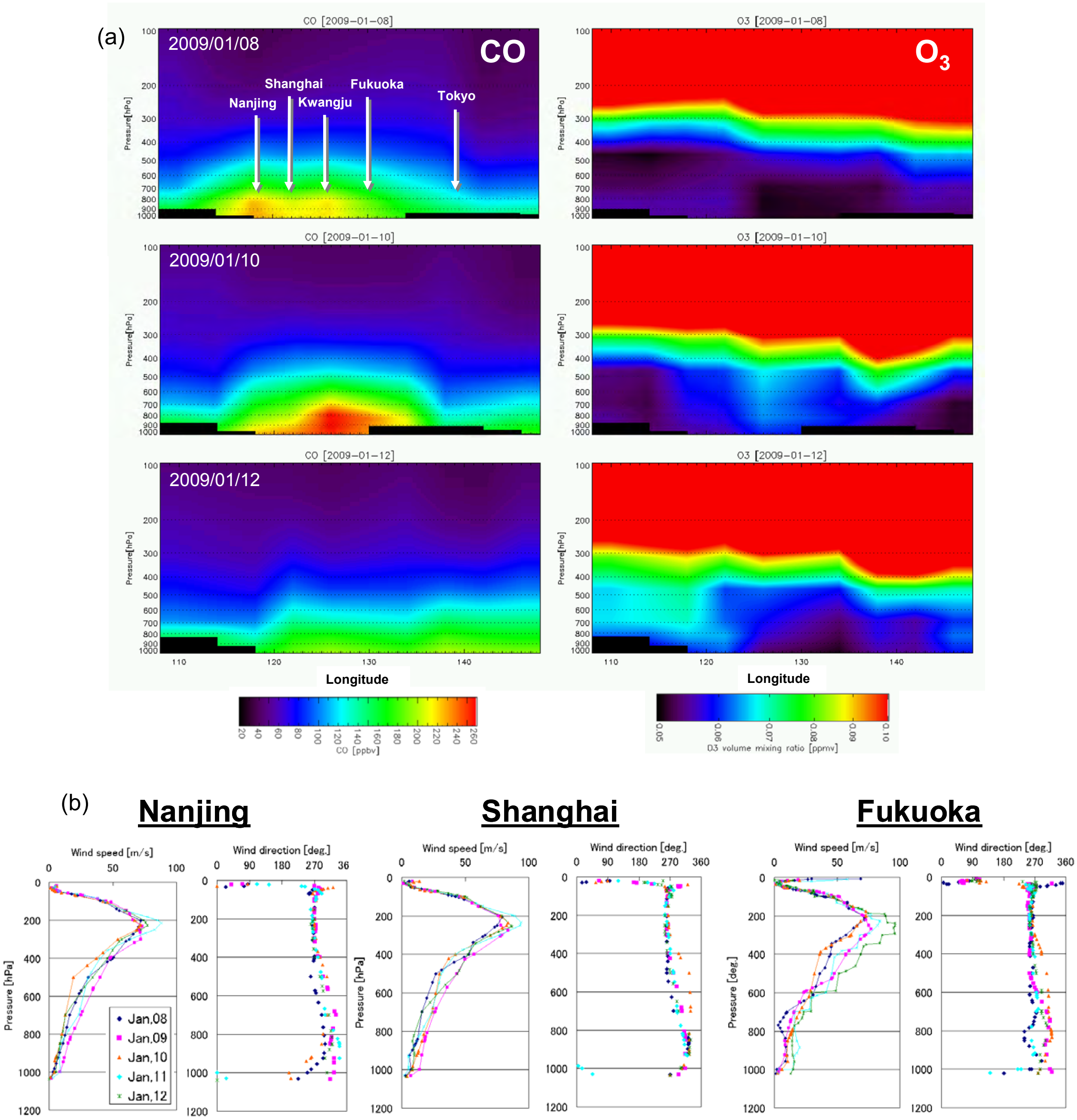

Figure 7. (a) The longitude-time cross section of CO and ozone for latitudinal band (zone1) from January 8 to January 12, 2009. (b) Profiles of wind speed and wind direction in Nanjing, Shanghai and Fukuoka at 12UTC on each day.

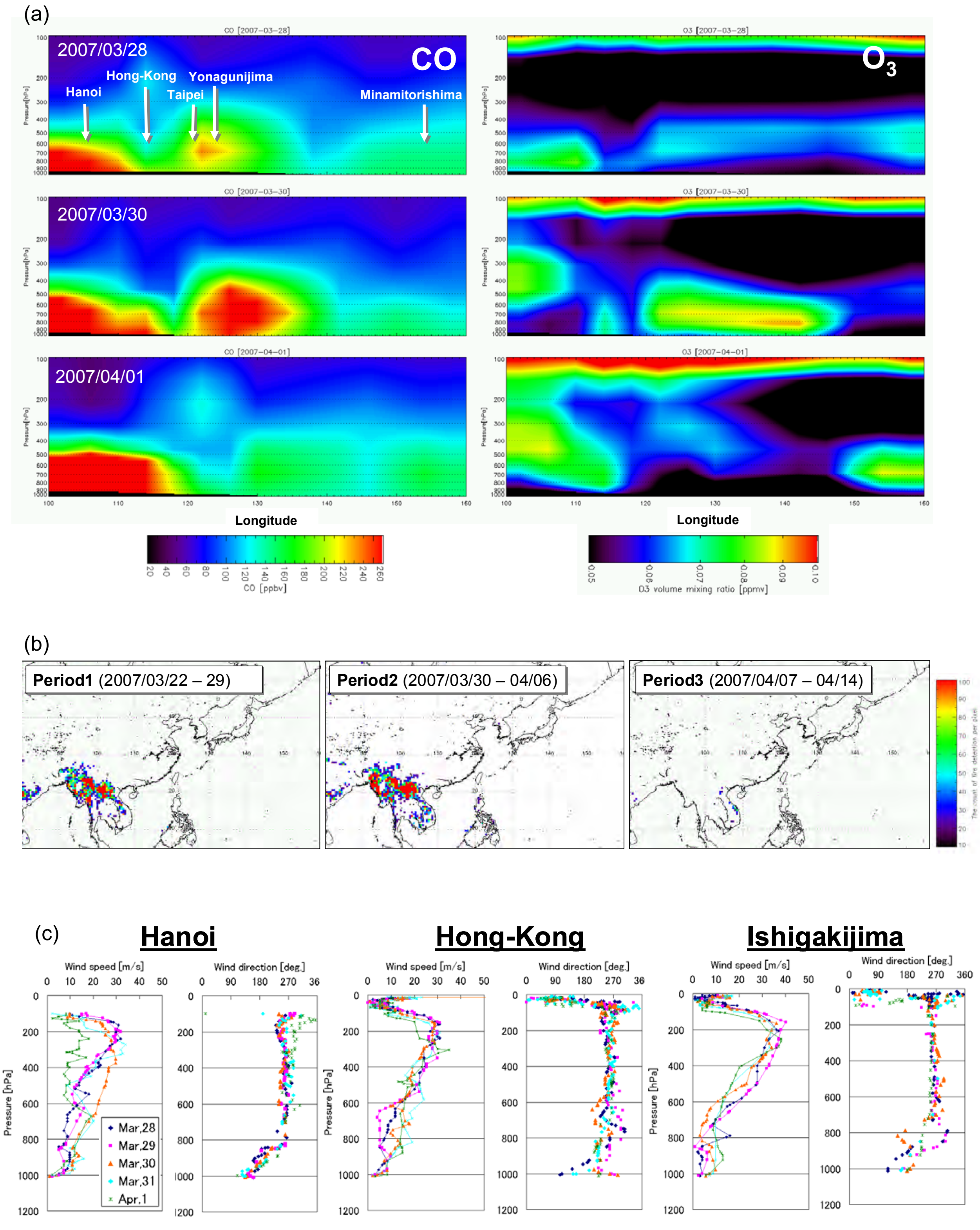

Figure 8. (a) The longitude-time cross section of CO and ozone for latitudinal band (zone2) from March 28 to April 1, 2007.
(b) MODIS CMG Fire product (MYD14C8H) in East Asia from March 3 to April 14, 2007 (8 days composite).
(c) Profiles of wind speed and wind direction in Nanjing, Shanghai and Fukuoka at 12UTC on each day.

4. DISCUSSION

As discussed in section3, the pollutant transport is controlled by airflow in troposphere. In order to monitor the atmospheric condition at fine intervals, we propose the creation of dataset using different satellite. It takes advantage of bridging the temporal-spatial gap.

Aura's orbit advances 22° westward and, it is back at same point after 16 days (233 orbits). Here, we instance the case of GOSAT (The Greenhouse gases Observing SATellite), which was launched on JAXA H-IIA Launch Vehicle No.15 in January 23, 2009.

The observation instrument onboard GOSAT is called the TANSO-FTS (Thermal And Near-infrared Sensor for carbon Observation - Fourier Transform Spectrometer). TANSO-FTS detects the short wave infrared (SWIR) reflected on the Earth's surface as well as the thermal infrared (TIR) radiated from the ground and the atmosphere. It is capable of covering three narrow bands (0.76, 1.6, and 2 μm) and a wide band (5.5-14.3 μm) with 0.2 cm^{-1} spectral resolution as shown in Table. 2.

The main target of TANSO-FTS is carbon dioxide and methane. Additionally, it could be detect other trace gases like ozone and nitrous oxide. As an example, we show TANSO-FTS weighting function and averaging kernel of these gases in Figure 8. Each gas can retrieve with three or four vertical resolutions in troposphere.

Table 2. Spectral region of GOSAT / TANSO-FTS.

	Band1	Band2	Band3	Band4
[μm]	0.758-0.775	1.56-1.72	1.92-2.08	5.56-14.3
[cm^{-1}]	13200-12900	6400-5800	5200-4800	2000-700

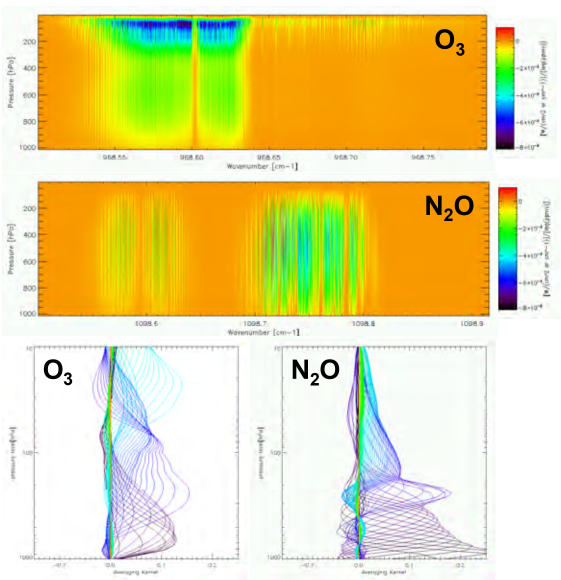

Figure. 8. TANSO-FTS weighting function of ozone and nitrous oxide (above). TANSO-FTS averaging kernel of each gases (below).

GOSAT orbit the earth in about 100 minutes at an altitude of approximately 666 km and return to the same orbit in three days show in Table 3. There are five pointing modes (1, 3, 5, 7 and 9) for TANSO-FTS observation over lattice points, depending on the number of scan in cross-track direction. It leads the advantage of wide observation range.

Figure 9 shows one-day orbit of Aura and GOSAT. If we combined these data, we could make higher-accuracy dataset by combing different satellite data.

Table 3. Orbital parameter of GOSAT.

Parameters	***Description***
Orbit type	Sun-synchronous
Altitude	666km at Equator
Inclination angle	98.06 deg.
Orbits/day	14+2/3 revolutions/day
Orbits/recurrence	44 revolutions/3day
Descending node time	13hours±15 min.

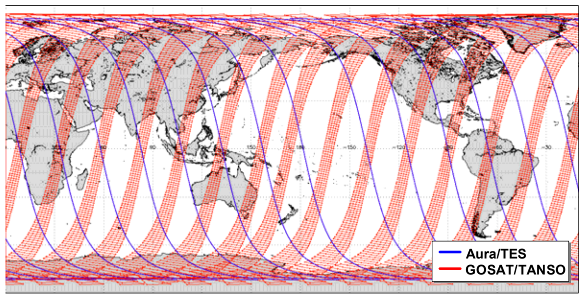

Figure 9. One-day orbit of Aura and GOSAT in the daytime.

5. SUMMARY

In this study, we analyzed a spatiotemporal dynamics of CO in East Asia using the data of recent years from 2006 to 2009. The regional scale of survey has revealed that the high CO events which exceed 300 ppbv in East Asia is not increasing yearly, but in 2007 is noticeable on emergence of high concentration.

In analysis of time trend of CO profile, the big city like Shanghai, Hong-Kong and Hanoi occasionally shows high concentration of CO in lower troposphere. These sources are thought to be an anthropogenic (factory, transport and domestic) and biomass burning. Sometimes, the high level of CO transport to Japan by cyclone or westerly wind and induced an anthropogenic ozone genesis.

Additionally, for the approaching of atmospheric condition in troposphere, we will propose the combine of different orbital satellite data.

Acknowledgements.

The authors are grateful to Jet Propulsion Laboratory, California Institute of Technology for allowing us to use the TES data and NASA/University of Maryland for MODIS CGM Fire Products. We are also indebt to Japan Meteorological Agency for providing ground-based observational data (via ftp site of WDCGG (The World Data Centre for Greenhouse Gases)), sonde data and meteorological chart.

REFERENCES

Bowman, K. W., D. B. A. Jones, J. A. Logan, H. Worden, F. Boersma, S. Kulawik, R. Chang, G. Osterman, and J. Worden: The zonal structure of tropical O3 and CO as observed by the Tropospheric Emission Spectrometer in November 2004. Part II. Impact of surface emissions on O3 and its precursors, *Atmos. Chem. Phys.*, 9, 3563-3582, June 3, 2009.

Giglio, L., Descloitres, J., Justice, C.O., Kaufman, Y. : An enhanced contextual fire detection algorithm for MODIS. *Remote Sensing of Environment*, 87:273-282, 2003.

Liang, Q., L. Jaeglé, D. A. Jaffe, P. Weiss, A. Heckman, and J. Snow: Long-range Transport to the Northeast Pacific: Seasonal variations and transport pathways, *J. Geophys. Res.*, 109, D23S07, doi:10.1029/2003JD004402, 2004.

Ohara,T., Akimoto,H., Kurokawa,J., Horii, N., Yamaji, K., Yan, X., and Hayasaka, T.: An Asian emission inventory of anthropogenic emission sources for the period 1980–2020, *Atmos. Chem. Phys.*, 7, 4419–4444, 2007.

Tanimoto,H., Sawa,Y., Yonemura, S., Yumimoto, K., Matsueda, H., Uno,I., Hayasaka, T., Mukai, H., Tohjima. Y., Tsuboi, K. and Zhang, L.: Diagnosing recent CO emissions and springtime O3 evolution in East Asia using coordinated ground-based observations of O3 and CO during the East Asian Regional Experiment (EAREX) 2005 campaign, *Atmos. Chem. Phys. Discuss*, 3525-3561, 2008.

Turquety, S., Clerbaux, C., Law, K., Cozic, A.,. Szopa,S., Hauglustaine, D. A., Hadji-Lazaro, J., Schrijver, H., Boone, C. D., Bernath, P. F., Edwards, D. P.: CO emission and export from Asia: an analysis combining complementary satellite measurements (MOPITT, SCIAMACHY and ACE-FTS) with global modeling, *Atmos. Chem. Phys.*, 8, 5187-5204, 2008.

Weiss-Penzias, P., D. A. Jaffe, L. Jaeglé, and Q. Liang :Influence of long-range-transported pollution on the annual and diurnal cycles of carbon monoxide and ozone at Cheeka Peak Observatory,*J. Geophys. Res*., 109, D23S14, doi:10.1029/2004JD004505, 2004.

Zhang, L., D. J. Jacob, K. W. Bowman, J. Logan, S. Turquety, R. C. Hudman, Q.Li, R. Beer, H. M. Worden, J. R. Worden, C. P. Rinsland, S. S. Kulawik, M.C. Lampel, M. W. Shephard, B. M. Fisher, A. Eldering, and M. A. Avery: Ozone-CO correlations determined by the TES satellite instrument in continental outflow regions, *Geophys. Res. Lett.*, 33, L18804, doi:10.1029/2006GL026399, 2006.

Zhang, L., D. J. Jacob, K. F. Boersma, D. A. Jaffe, J. R. Olson, K. W. Bowman,J. R. Worden, A. M. Thompson, M. A. Avery, R. C. Cohen, J. E. Dibb, F. M.Flocke, H. E. Fuelberg, L. G. Huey, W. W. McMillan, H. B. Singh, and A. J.Weinheimer: Transpacific transport of ozone pollution and the effect of recent Asian emission increases on air quality in North America: an integrated analysis using satellite, aircraft, ozonesonde, and surface observations, *Atmos. Chem. Phys.*, 8, 6117-6136, 2008.